Engineering Hyperactive Variants of Human Deoxyribonuclease I by Altering Its Functional Mechanism

Clark Q. Pan and Robert A. Lazarus*

Department of Protein Engineering, Genentech, Inc., 460 Point San Bruno Boulevard, South San Francisco, California 94080

Received December 3, 1996; Revised Manuscript Received March 14, 1997[⊗]

ABSTRACT: Human deoxyribonuclease I (DNase I), an enzyme used to treat cystic fibrosis patients, has been engineered to more effectively degrade double-stranded DNA to lower molecular weight fragments by altering its functional mechanism from the native single-stranded nicking pathway to a much more efficient one which results in increased double-stranded scission. By introducing positively charged amino acids at DNase I positions that can interact favorably with the proximal negatively charged phosphate groups of the DNA, we have created a hyperactive variant with ∼35-fold higher DNA-degrading activity relative to wild type. This enhancement can be attributed to both a decrease in K_m and an increase in V_{max}. Furthermore, unlike wild-type DNase I, the hyperactive variants are no longer inhibited by physiological saline. Replacement of the same positions with negatively charged amino acids greatly reduced DNA cleavage activity, consistent with a repulsive effect with the neighboring DNA phosphates. In addition, these variants displayed similar activities toward a small synthetic substrate, *p*-nitrophenyl phenylphosphonate, suggesting that the difference in DNA cleavage activity is due to the interaction of the engineered charged residues with the DNA phosphate backbone rather than any change in catalytic machinery. Finally, experiments involving the repair of DNase I digested DNA with T4 DNA ligase and the Klenow fragment of DNA polymerase I suggest that single-stranded gaps are introduced by the hyperactive variants. Thus, the increased functional activity of the hyperactive variants may be explained in part by a shift toward a processive DNA nicking mechanism, which leads to a higher frequency of double-stranded breaks.

In addition to its fundamental role in biology, DNA is also involved in the pathogenesis of a number of diseases. In patients with cystic fibrosis (CF),[1] a defective CF transmembrane conductance regulator gene results in viscous airway secretions containing high concentrations of DNA, which is derived from leukocytes in response to the persistent bacterial infections associated with this disease (Boat et al., 1989; Collins, 1992; Quinton, 1990). The ability of recombinant human DNase I to degrade DNA to lower molecular weight forms, thus reducing the viscoelasticity of sputum, has led to improved lung function and reduced respiratory exacerbations (Fuchs et al., 1994; Ramsey et al., 1993; Shak et al., 1990). In addition, the presence of antibodies to nuclear antigens including DNA is the hallmark of systemic lupus erythematosus (SLE), an autoimmune disease that affects multiple organ systems; antibodies directed against double-stranded DNA appear to play a prominent role in lupus nephritis (Kotzin & O'Dell, 1995). The use of DNase I for destruction of the DNA antigen has been investigated in a murine model of SLE with encouraging results (Lachmann, 1996; Macanovic et al., 1996).

From a protein engineering perspective, the ability to improve the native activity of an enzyme represents a significant challenge. In the case of DNase I, engineering the wild-type enzyme to one with higher activity may result in improved clinical benefit for CF and SLE patients. We have recently shown that G-actin is a significant inhibitor of DNase I in CF sputum and that actin-resistant variants are 10−50-fold more potent than wild type in CF sputum (Ulmer et al., 1996). In the present work, we sought to engineer a substantially better enzyme with enhanced functional activity, i.e., one that more effectively reduces DNA length under physiological conditions.

DNase I is an endonuclease that catalyzes the hydrolysis of double-stranded DNA predominantly by a single-stranded nicking mechanism under physiological conditions when both Ca^{2+} and Mg^{2+} ions are present (Campbell & Jackson, 1980). However, the reduction of DNA length would be far more efficient if the enzyme undertook a functional mechanism that results in increased double-stranded breaks; a mathematical treatment of these situations has been described (Cowan et al., 1987). Effective double-stranded scission could result either from a mechanism where individual nicks were introduced in close proximity on both strands or by a processive nicking mechanism that creates DNA gaps instead of nicks, thus increasing the probability of double-stranded breaks.

We reasoned that, by increasing the affinity of DNase I for DNA, we could prolong the half-life of the DNA−DNase I complex and potentially favor either of these more efficient degradation pathways. To improve DNA affinity, we have selected 11 positions at the DNA−DNase I interface for

* To whom correspondence should be addressed. Tel: 415-225-1166. Fax: 415-225-3734.

[⊗] Abstract published in *Advance ACS Abstracts,* May 1, 1997.

[1] Abbreviations: DNase I, deoxyribonuclease I; CF, cystic fibrosis; SLE, systemic lupus erythematosus; EDTA, ethylenediaminetetraacetic acid; TBE, Tris−borate−EDTA; Hepes, *N*-2-(hydroxylethyl)piperazine-*N*′-2-ethanesulfonic acid; NPPP, *p*-nitrophenyl phenylphosphonate. One letter codes are used to represent naturally occurring L-amino acids. When referring to mutants, the wild-type amino acid is followed by the residue number and the new amino acid as in E13R; DNase I variants with multiple mutations are denoted with a colon between the individual mutations such as E13R:N74K or 13R:74K.

S0006-2960(96)02960-1 CCC: $14.00

substitution with basic amino acid residues. The engineered positive charges were designed to generate attractive interactions with the negatively charged phosphates on the DNA backbone. Additionally, we reasoned that we could potentially overcome the significant inhibition of DNase I by physiological saline by employing the same strategy. Eight out of the eleven selected positions resulted in variants having hyperactivity for DNA scission. The combination of three such positions created a hyperactive DNase I variant with ~35-fold higher DNA cleavage activity than wild type as well as one that is no longer inhibited by physiological saline.

MATERIALS AND METHODS

Mutagenesis, Expression, and Characterization. Site-directed mutagenesis, expression in human 293 cell culture, human DNase I ELISA, and actin binding ELISA measurements were carried out essentially as previously described (Ulmer et al., 1996). The actin binding affinity of all of the variants described herein was the same as wild type, implying that their overall structural integrity remained intact.

Kinetic Measurements. Kinetic assays were based on the Kunitz hyperchromicity assay (Kunitz, 1950). Culture media from 293 cells transfected with wild-type or variant DNase I were diluted 2−50 fold into a solution containing 10−400 μg/mL calf thymus DNA (Sigma) in 25 mM Hepes, pH 7, 1 mM $MgCl_2$, 2.5 mM $CaCl_2$, and 150 mM NaCl at room temperature in a final volume of 150 μL in a 96-well plate. The subsequent increase in absorbance at 260 nm was monitored for 6 min with a Molecular Devices Spectra Max 250 spectrophotometer. No activity was detected in 1:2 diluted mock-transfected media. Plots of initial rates of A_{260} increase versus DNA concentration were hyperbolic for most variants, and the data were fit to the Michaelis−Menten equation to generate apparent K_m and V_{max} kinetic values. While the absolute steady-state values cannot be reported with commonly used units due to the nature of the polymeric substrate, the unknown number and type of different substrate binding sites, and the unclear relationship between the absorbance signal and the actual catalytic events (Doherty et al., 1995), a comparison of the apparent K_m and V_{max} values between mutants and wild type provides useful information. For the salt inhibition assay (Figure 5B), the DNA concentration was fixed at 300 μg/mL and the amount of NaCl varied from 0 to 400 mM.

Plasmid Digestion Assay in Native Agarose Gel. In a final volume of 160 μL, 30 μg/mL supercoiled pBR322 plasmid DNA (New England Biolabs) or 25 μg/mL linearized pBR322 (*Eco*RI-digested and purified by phenol−chloroform extraction and ethanol precipitation) was incubated with >1000-fold diluted culture media in the presence of 25 mM Hepes, pH 7, 100 μg/mL bovine serum albumin, 1 mM $MgCl_2$, and 2.5 mM $CaCl_2$, with varying NaCl concentrations at room temperature. At various time intervals, 30 μL aliquots of the reaction mix were quenched with 25 mM EDTA, 6% glycerol, xylene cyanol, and bromophenol blue and loaded directly onto a 0.8% agarose gel. The gel was run overnight at ~1 V/cm in TBE (90 mM Tris−borate and 2 mM EDTA), stained with ethidium bromide, and individual bands were quantified with a Molecular Dynamics Model 575 FluorImager. The overall activity was measured as the initial rate of disappearance of supercoiled or linear substrate. The linear to relaxed ratio was also determined from the initial rates of appearance of linear and relaxed products. Mock-transfected media diluted 100-fold showed no background activity.

Plasmid Digestion Assay in Denaturing Agarose Gel. *Eco*RI-linearized plasmid pBR322 (30 μg/mL) was incubated with diluted culture media in the presence of 25 mM Hepes, pH 7, 1 mM $MgCl_2$, and 2.5 mM $CaCl_2$, at room temperature in a final volume of 550 μL. At various times, 60 μL aliquots were quenched with 25 mM EDTA, 6% glycerol, xylene cyanol, and bromophenol blue. One-third of this mix was run on a 0.8% native agarose gel in TBE to follow double-stranded cleavage. The other two-thirds were mixed with NaOH to a final concentration of 50 mM and run on a 0.8% denaturing agarose gel in 50 mM NaOH to monitor single-stranded nicking. Both gels were run at ~0.5 V/cm overnight, stained with ethidium bromide, and analyzed with a Molecular Dynamics Model 575 FluorImager. The activity was measured as the initial rate of disappearance of linear DNA substrate.

^{32}P-Labeled Fragment Digestion. *Eco*RI-linearized plasmid pBR322 was radiolabeled at the 3′-end with the Klenow fragment of DNA polymerase I (U.S. Biochemicals) and [α-^{32}P]dATP (Amersham) or at the 5′-end with T4 Kinase (U.S. Biochemicals) and [γ-^{32}P]ATP (Sambrook et al., 1989), followed by digestion with *Ssp*I and polyacrylamide gel purification of the 190mer restriction fragment. The uniquely end-labeled 190mer fragment at ~0.5 μg/mL concentration was treated with diluted culture media from DNase I transfected 293 cells for 5 min at room temperature in the presence of 25 mM Hepes, pH 7, 1 mM $MgCl_2$, and 1 mM $CaCl_2$ in a final volume of 18 μL and quenched with 0.5 μM G-actin (Sigma). The quenched reaction mix (12 μL) was then added to ~100 units of T4 ligase (New England Biolabs), 1 mM ATP, and 0.5 mM each of dNTP, 10 mM Tris, pH 7.5, 5 mM $MgCl_2$, and 2 mM dithiothreitol. The ligase reaction mix (6 μL) was added to ~1.5 units of the Klenow fragment of DNA polymerase I. All three 6 μL reaction mixes were incubated at 37 °C for 30 min, followed by quenching with 24 μL of 15 mM EDTA and deionized formamide. The G + A marker was generated by chemical modification of the end-labeled 190mer by the Maxam−Gilbert method (Sambrook et al., 1989). A 12% denaturing polyacrylamide gel containing 10 μL of each mix was run, dried, and incubated with a Fuji phosphoimaging plate (type BAS-III), which was then scanned with a Fuji phosphoimager (BAS2000).

p-Nitrophenyl Phenylphosphonate Assay. DNase I hydrolytic activity on a small molecule substrate, p-nitrophenyl phenylphosphonate (NPPP) (Sigma), was determined by monitoring the increase in A_{405} as a result of the generation of *p*-nitrophenol. Reactions were carried out with 10 mM NPPP incubated with culture media in the presence of 60 mM Hepes, pH 7, 50 mM $MgCl_2$, and 50 mM $CaCl_2$. The activity of DNase I transfected media was corrected for background activity detected in mock-transfected media.

RESULTS

Design of Hyperactive DNase I Variants. Positively charged residues at selected positions of DNase I were introduced on the basis of a model of human DNase I complexed with DNA (Figure 1A). The model of the complex was generated by superposition of human DNase

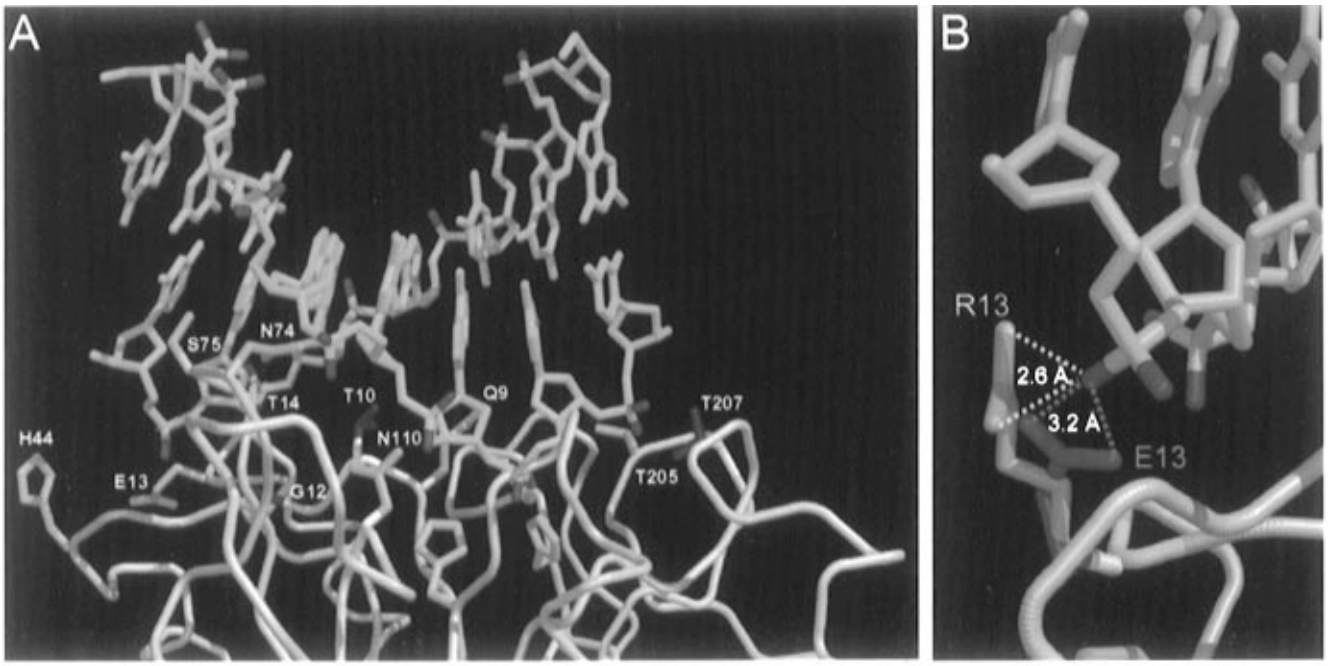

FIGURE 1: Model of the human DNase I−DNA complex. (A) Eleven residues at the DNA binding interface of the human DNase I−d(GGTATACC)$_2$ complex that were altered are labeled and colored in blue; the model was derived by superposition of human DNase I (Wolf et al., 1995) with the bovine DNase I−octamer complex (Weston et al., 1992). Those eight positions that yielded hyperactivity are denoted in lighter blue while the other three are in darker blue. The catalytic histidines at positions 134 and 252 are depicted in yellow. The phosphate oxygens of the DNA (green) are highlighted in red. (B) Close-up view of the interaction of residue 13 with DNA. The native Glu (red) and the variant Arg (blue) have been modeled to interact with the phosphate oxygens (red) of the DNA. The figures were made using MidasPlus (Ferrin et al., 1988).

I, recently solved at 2.2 Å resolution (Wolf et al., 1995), with the bovine DNase I−octamer complex (Weston et al., 1992); the overall RMS deviation for main chain atoms was 0.56 Å. Eleven positions were chosen because their C_α to C_β trajectories are directed toward the DNA, and the positively charged amines of the engineered Arg or Lys can be modeled to be within 3 Å of the negatively charged phosphates in the DNA backbone. Figure 1B demonstrates our selection process for residue 13. The negatively charged carboxylates of the wild-type glutamic acid can be modeled to be close enough to the negatively charged DNA phosphate to yield repulsive interactions, while the positively charged amines of the engineered arginine can also reach the same phosphate to generate attractive interactions. To test our strategy, we have constructed site-directed mutants of human DNase I, expressed them in human 293 cells, and characterized their activities in several different assays.

Kinetic Characterization. Kinetic values for the DNase I variants were obtained using the DNA hyperchromicity assay, which measures an increase in the absorbance at 260 nm as DNA is degraded (Kunitz, 1950). Plots of initial velocity vs substrate concentration yielded hyperbolic curves for wild-type DNase I and most variants (Figure 2), allowing the extraction of apparent K_m and V_{max} values using the Michaelis−Menten equation (Table 1). Removal of the negative charge at position 13 of DNase I with an alanine substitution (E13A) resulted in a significant increase in activity (Figure 2A); charge reversals at this position (E13K or E13R) produced even higher activity. Retaining the negative charge (E13D) had minimal effect. Most of the elevated activities of the positively charged variants could be ascribed to a decrease in K_m (Table 1), suggesting that their hyperactivities were mainly due to stronger DNA binding affinities. Two notable exceptions were Q9R and

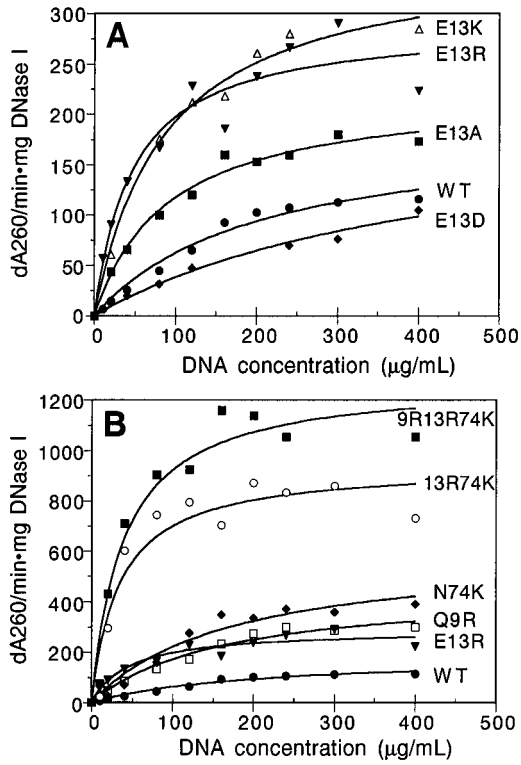

FIGURE 2: DNA hyperchromicity assay of human DNase I variants. Calf thymus DNA at the specified DNA concentrations is treated with DNase I variants, and the increase in absorbance at 260 nm as a result of DNA degradation is followed. The initial velocity is plotted against the DNA concentration. (A) Mutations that affect charge at position 13 of DNase I. (B) Individual and cumulative effects of Q9R, E13R, and N74K variants of DNase I.

N74K, which had an increased V_{max} without affecting K_m. The increase in V_{max} for Q9R can be explained by the fact

Table 1: DNA Digestion Activity of Human DNase I Variants[a]

	DNA hyperchromicity assay			linear DNA	supercoiled DNA	
variants	$1/K_m$	V_{max}	V_{max}/K_m	activity	L/R	activity
wild type	1.0 ± 0.1	1.0 ± 0.1	1.0	1.0 ± 0.1	1.0	1.0 ± 0.01
Q9R	0.9 ± 0.2	2.8 ± 0.4	2.6	3.5 ± 0.4	2.3	3.4 ± 0.5
E13D	0.8 ± 0.1	0.8 ± 0.1	0.6	0.6 ± 0.1		
E13A	2.3 ± 0.3	1.2 ± 0.1	2.7	2.2 ± 0.6		
E13K	2.5 ± 0.4	1.8 ± 0.1	4.5	3.9 ± 0.1		
E13R	4.3 ± 1.4	1.5 ± 0.1	6.5	6.0 ± 0.5	5.4	2.2 ± 0.01
T14D				0.07		
T14K	2.3 ± 0.9	1.1 ± 0.2	2.5	4.2 ± 0.1	4.7	2.9 ± 0.8
T14R	2.1 ± 0.8	0.7 ± 0.1	1.5	3.5 ± 0.7		
H44E				0.05		
H44K	2.3 ± 0.5	1.1 ± 0.1	2.5	2.0 ± 0.4	2.3	1.8 ± 0.3
H44R	1.7 ± 0.2	1.0 ± 0.1	1.7	3.6 ± 0.5		
N74E				0.07		
N74K	1.3 ± 0.4	3.6 ± 0.5	4.7	6.0 ± 0.1	4.7	7.3 ± 1.0
N74R	2.6 ± 0.8	3.1 ± 0.3	8.1	4.1 ± 0.8		
N110R				10.4 ± 0.4	2.3	7.9 ± 1.7
T205D				<0.005		
T205K	2.4 ± 0.8	2.1 ± 0.4	5.0	4.7 ± 0.2	5.4	2.8 ± 0.7
T205R	3.0 ± 1.2	1.0 ± 0.1	3.0	2.3 ± 0.3		
E13R:N74K	5.0 ± 1.7	5.3 ± 0.5	26.5	26.7 ± 4.1	12.3	6.9 ± 1.6
Q9R:E13R:N74K	4.9 ± 1.3	7.0 ± 0.4	34.3	38.3 ± 1.2	16.5	6.3 ± 2.2

[a] Experiments were carried out under physiological conditions of 1 mM Mg^{2+}, 2.5 mM Ca^{2+}, and 150 mM NaCl at pH 7. All values are normalized relative to those of wild type, which has a K_m of 229 ± 33 μg/mL DNA ($n = 6$), V_{max} of 168 ± 18 A_{260} units min^{-1} (mg of DNase I)$^{-1}$ ($n = 6$), linear DNA cleavage activity of 23 ± 3 mg of DNA min^{-1} (mg of DNase I)$^{-1}$ ($n = 6$), and a linear/relaxed product ratio (L/R) of 0.010 for supercoiled DNA digestion with overall loss of the supercoiled substrate DNA at 1200 ± 43 mg of DNA min^{-1} (mg of DNase I)$^{-1}$ ($n = 2$). The number of separate experiments done is denoted by *n*.

that Arg9 of bovine DNase I is near the scissile bond and has been proposed to stabilize the pentavalent transition state (Weston et al., 1992); the reason for the increase in V_{max} for N74K is not readily apparent. Effects of single mutations of E13R and N74K are additive, and their combination with Q9R produced the most hyperactive variant Q9R:E13R:N74K, which is ~35-fold more active than native DNase I under physiological conditions (Figure 2B and Table 1).

Supercoiled Plasmid Digestion Assay. The DNA hyperchromicity data suggested that most of the hyperactive variants have stronger affinities for DNA and thus may stay on the DNA longer, potentially allowing some double-stranded DNA scission. To test this, we used supercoiled plasmid pBR322 as a substrate for DNA cleavage. A single nick on one of the two supercoiled DNA strands results in the formation of a relaxed circle which can subsequently be converted to linear DNA if it is nicked on the other strand at the same position. Wild-type human DNase I cleaves double-stranded DNA via a nicking mechanism as evidenced by the initial conversion of supercoiled substrate to relaxed circle; the appearance of the linear DNA product is apparent only after multiple nicks (Figure 3A), in agreement with previous studies on bovine DNase I (Laskowski, 1971). The introduction of a positive charge in human DNase I created variants (E13R and N74K) that were hyperactive and produced significantly more linear products than did the native enzyme; the linear to relaxed product ratio was even greater for the E13R:N74K double mutant (Figure 3A, Table 1).

Linear Plasmid DNA Digestion Activity. Because double-stranded DNA scission is so much more efficient than single-stranded nicking for reducing the length of DNA, data from supercoiled plasmid cleavage predicts that these positively charged DNase I variants should be more active than wild type in degrading linearized plasmid DNA. As illustrated in Figure 3B, these variants were indeed hyperactive relative to wild type, especially under physiological conditions of 150 mM NaCl. Interestingly, in the absence of NaCl, the E13R:N74K double mutant actually shows a relative decrease in the DNA-nicking activity as evidenced by the slower disappearance of the supercoiled DNA substrate (Figure 3A, top panel), consistent with tighter substrate binding and slower release of the nicked product (see below). This implies that it is not the total number, but rather the type of catalytic events, i.e., double-stranded scission, that imparts hyperactivity. The double mutant E13R:N74K has more than 20-fold higher functional activity than native DNase I in degrading linear DNA (Figure 3B, bottom panel).

We have also assessed the single-stranded nicking of linearized plasmid DNA by analyzing the products on a denaturing agarose gel (Sambrook et al., 1989). Double-stranded scission from the same reaction was detected separately on a native agarose gel. In the absence of NaCl, the single-stranded nicking activity on linear DNA of the E13R:N74K double mutant is less than that of the wild-type DNase I (Figure 4, top panel), consistent with the supercoiled plasmid DNA digestion assay (Figure 3A, top panel). However, the double-stranded cutting activity of the E13R:N74K mutant was greater than that of the wild type (Figure 4, bottom panel; Figure 3B, top panel). The ratio of double-stranded cutting to single-stranded nicking rates for E13R:N74K is ~7-fold higher than that of the wild type. Taken together, these results suggest that the additional basic side chains of the variants may provide the enzyme with higher DNA affinity, which favors a pathway involving double-stranded scission.

The supercoiled and linear DNA cleavage activities for seven single positively charged mutants relative to wild type under physiological conditions are listed in Table 1. In each case, the increase in activity of linear DNA scission is accompanied by a similar increase in the ratio of linear to relaxed product derived from the supercoiled substrate. The

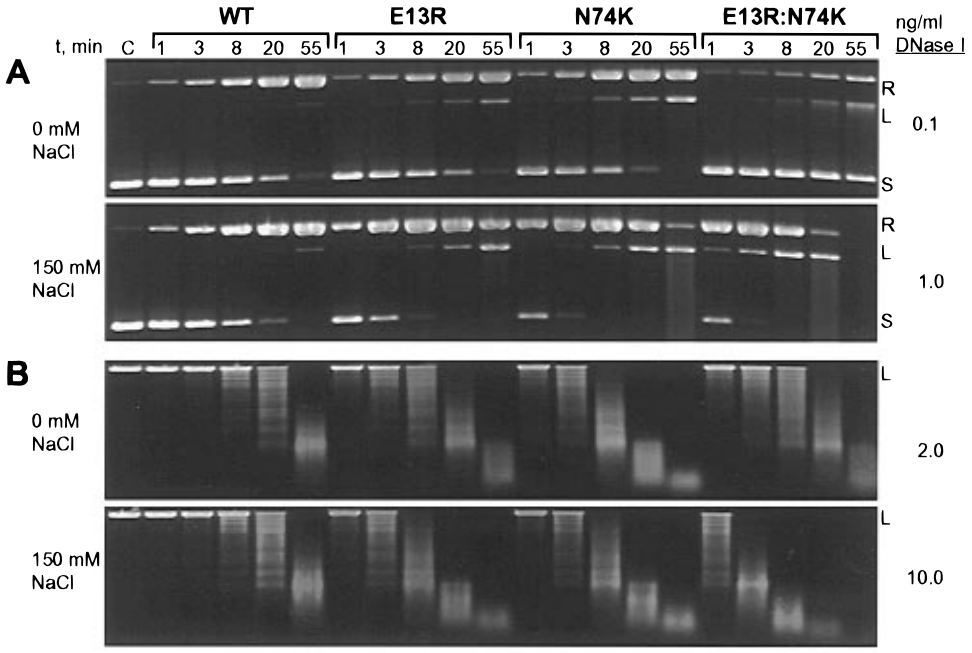

FIGURE 3: Plasmid DNA digestion by human DNase I variants. (A) Supercoiled pBR322 substrate with a low level of relaxed circle background (first lane, "C" for control) is incubated with 0.1 ng/mL wild-type, E13R, N74K, and E13R:N74K DNase I in a solution containing no NaCl from 1 to 55 min (top panel). The linear product (L) runs in between the slower moving relaxed product (R) and the faster moving supercoiled substrate (S). In the bottom panel, 150 mM NaCl is included in the reaction mix, and the DNase I concentration is correspondingly increased to 1 ng/mL. (B) The *Eco*RI-linearized pBR322 substrate is degraded by 2 ng/mL DNase I in the presence of 0 mM NaCl (top panel) or 10 ng/mL DNase I when 150 mM NaCl is added (bottom panel). The figures were made using Adobe Photoshop 3.0.5.

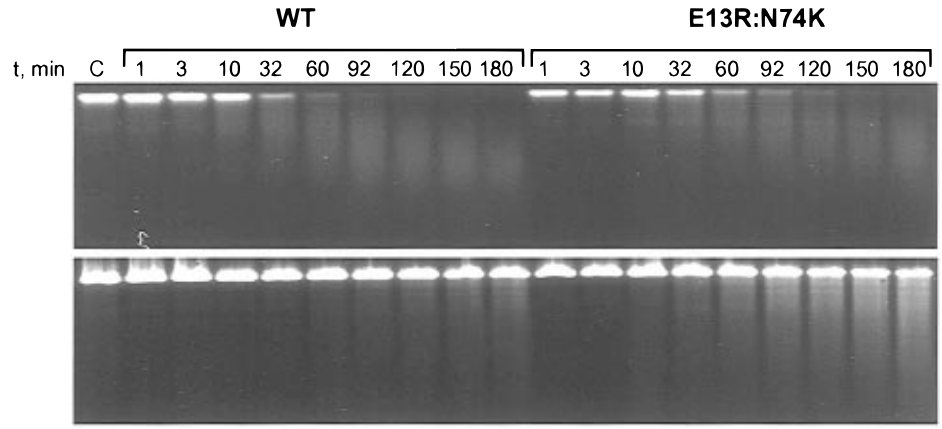

FIGURE 4: Linear plasmid DNA digestion by human DNase I variants. The *Eco*RI-linearized pBR322 substrate is degraded by 0.1 ng/mL DNase I in the absence of NaCl. The products of DNA cleavage were analyzed on a denaturing agarose gel to visualize single-stranded nicking (top panel) or a native agarose gel to monitor double-stranded scission (bottom panel).

effect of single mutations are additive as seen in the double (E13R:N74K) and triple (Q9R:E13R:N74K) mutants. The linear DNA digestion data are in excellent agreement with the kinetic values for the DNase I variants obtained with the DNA hyperchromicity assay. Having a negative charge at these positions greatly reduced linear DNA degradation activity, consistent with them being proximal to the negatively charged DNA phosphate backbone (Table 1). Four other positions were also replaced with lysine. The activity of S75K was increased by only 50% while that of T207K was comparable to wild type. In agreement with the other hyperactive variants, S75K also showed an ~2-fold decrease in K_m and ~7-fold increase in the linear to relaxed product ratio in the presence of Ca^{2+} and Mg^{2+}. T10K and G12K possessed much lower activities than wild type, perhaps a result of disruptions of the protein−DNA interaction by the bulky side chain of lysine. In addition, the removal of a positive charge at the protein−DNA interface by R41A lowered the supercoiled plasmid nicking activity by over 100-fold; this agrees with data from bovine R41A, which has 0.5% V_{max}/K_m compared to wild type (Doherty et al., 1995). Furthermore, the linear to relaxed ratio for human R41A was reduced by 5-fold. The supercoiled nicking comparison of R41A and wild type was carried out in the presence of Mn^{2+} due to relatively poor expression of R41A coupled with its low activity using Mg^{2+}. The role of R41, which binds in the minor groove, has been suggested to ensure efficient catalysis by optimally positioning the scissile bond (Doherty et al., 1995).

Salt Effects on DNA Cleavage Activity. We have addressed the ionic effects on the DNA cleavage activity of the variants further since salt concentration plays a significant role in protein−DNA interactions (Misra et al., 1994; Record et al., 1978). Wild-type DNase I is highly sensitive to salt,

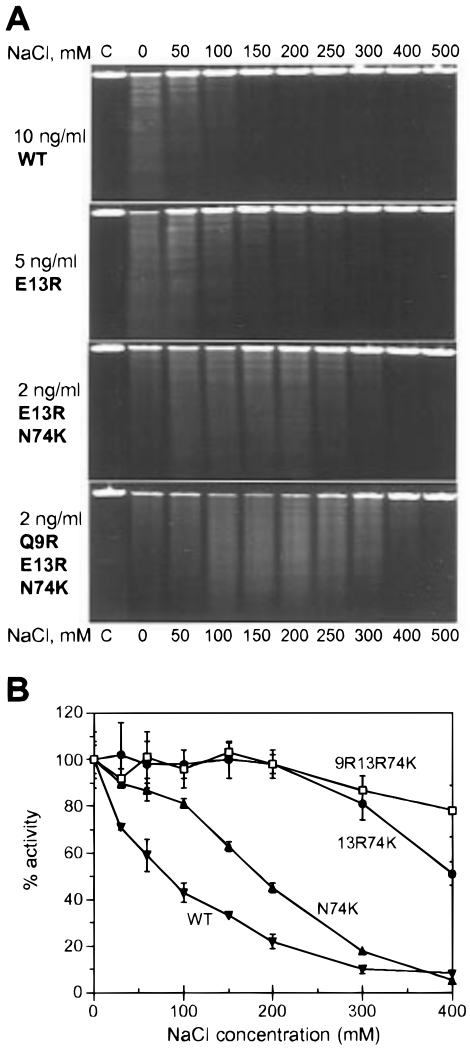

FIGURE 5: NaCl effect on DNA digestion by human DNase I variants. (A) *Eco*RI-linearized pBR322 DNA at 25 μg/mL is treated with wild-type, E13R, E13R:N74K, and Q9R:E13R:N74K DNase I at the specified concentrations in the presence of increasing NaCl concentrations and analyzed on a native agarose gel. (B) The DNA hyperchromicity assay is used to follow the digestion of calf thymus DNA at the near-saturating concentration of 300 μg/mL with DNase I at increasing NaCl concentrations. The activity at a particular NaCl concentration is divided by the activity for the same variant in the absence of NaCl to obtain the percent activity. The activities in the absence of NaCl for wild-type, N74K, E13R:N74K, and Q9R:E13R:N74K are 171 $\pm$ 10, 690 $\pm$ 5, 432 $\pm$ 36, and 506 $\pm$ 60 A_{260} units min^{-1} (mg of DNase I)$^{-1}$, respectively.

having ~50% and ~15% linear plasmid DNA cleavage activity at 60 and 150 mM NaCl, respectively (Figures 3 and 5A). With a single added positive charge (E13R), the salt concentration for 50% inhibition increases to ~110 mM; with two (E13R:N74K) and three (Q9R:E13R:N74K) additional basic residues, the optimal salt concentration is ~100 and ~150 mM, respectively (Figure 5A). In the absence of salt, wild-type DNase I may bind DNA with optimal affinity whereas the best hyperactive variants may bind to the DNA too tightly for effective catalysis. Upon addition of NaCl, the increased ionic strength should lower the substrate DNA binding affinity for DNase I, which results in significant inhibition of the native enzyme. However, in the case of the hyperactive variants, the increase in ionic strength likely permits a faster release of product DNA from the enzyme.

Data from the DNA hyperchromicity assay (Figure 5B) are consistent with that from the linear plasmid DNA cleavage assay (Figure 5A). In the hyperchromicity assay, the relative activity of DNase I at a particular NaCl concentration to that at 0 mM NaCl concentration is plotted against the NaCl concentration. Again, wild-type human DNase I is sharply inhibited by salt, with ~50% and ~30% hyperchromicity activity at 80 and 150 mM NaCl concentration, respectively. By adding one (N74K), two (E13R:N74K), or three (Q9R:E13R:N74K) positive charges to DNase I, the inhibitory effect by salt was progressively relieved. Both assays indicate that the optimal salt concentration for the most active variant Q9R:E13R:N74K is at the physiological saline concentration of 150 mM.

Digestion of a ^{32}P-Labeled 190 bp DNA Fragment. To analyze the products of DNase I cleavage at the nucleotide resolution, we used a uniquely end-labeled DNA fragment as substrate. Unlike ethidum bromide staining of DNA, end labeling allows an accurate quantitation of DNA fragments that have different length. The experimental conditions were controlled such that the wild-type DNase I and the hyperactive variant E13R:N74K yielded approximately the same number of nicks on the 190 bp uniquely end-labeled *Eco*RI−*Ssp*I fragment of pBR322 (Figure 6). The degradation pattern by the wild-type and the E13R:N74K mutant DNase I on the 5′-*Eco*RI end-labeled upper strand is shown in Figure 6B (lanes 2 and 3); a profile of the degradation pattern on the 3′-*Eco*RI end-labeled lower strand is illustrated in Figure 6C. The hyperactive variant showed no apparent change in sequence preference as compared to wild-type DNase I; however, it did result in a greater proportion of lower molecular weight products (Figure 6B,C). The shift to smaller sized products is consistent with the idea that the hyperactive variants processively nick along the same DNA strand, thus generating gaps in the DNA (Figure 6A). To test this idea, we used T4 ligase and the Klenow fragment of DNA polymerase I to repair the damage produced by DNase I. Almost all the nicks produced by wild-type DNase I were resealed by the ligase as shown by the disappearance of the degradation products (Figure 6B, lane 5). However, the degradation products created by the hyperactive E13R:N74K mutant remained upon ligase treatment (Figure 6B, lane 6) and disappeared only when the Klenow fragment and dNTPs were also included in the ligation reaction (Figure 6B, lane 9). These results suggest that wild-type DNase I generates nicks in the DNA while the hyperactive variants produce gaps that can only be sealed with ligase if they are first filled in with the Klenow fragment of DNA polymerase I (Figure 6A).

Hydrolysis of a Small Molecule Substrate. With the exception of Arg9, the positions chosen for basic residue replacement are relatively remote from the two catalytic histidines at the active site (Figure 1A) and should not affect DNase I activity using small molecule substrate analogs. Indeed, wild-type, T14K, N110R, E13R:N74K, and T205D human DNase I display similar activities of 1.0, 1.2, 0.8, 1.2, and 1.6 A_{405} units min^{-1} (mg of DNase I)$^{-1}$, respectively, using *p*-nitrophenyl phenylphosphonate as the substrate (Liao & Hsieh, 1988). The removal of one of the two catalytic histidines by the H134A mutation lowered the activity by more than 100-fold, indicating that the catalytic machinery for DNA cleavage is required for the hydrolysis of the small DNA analog.

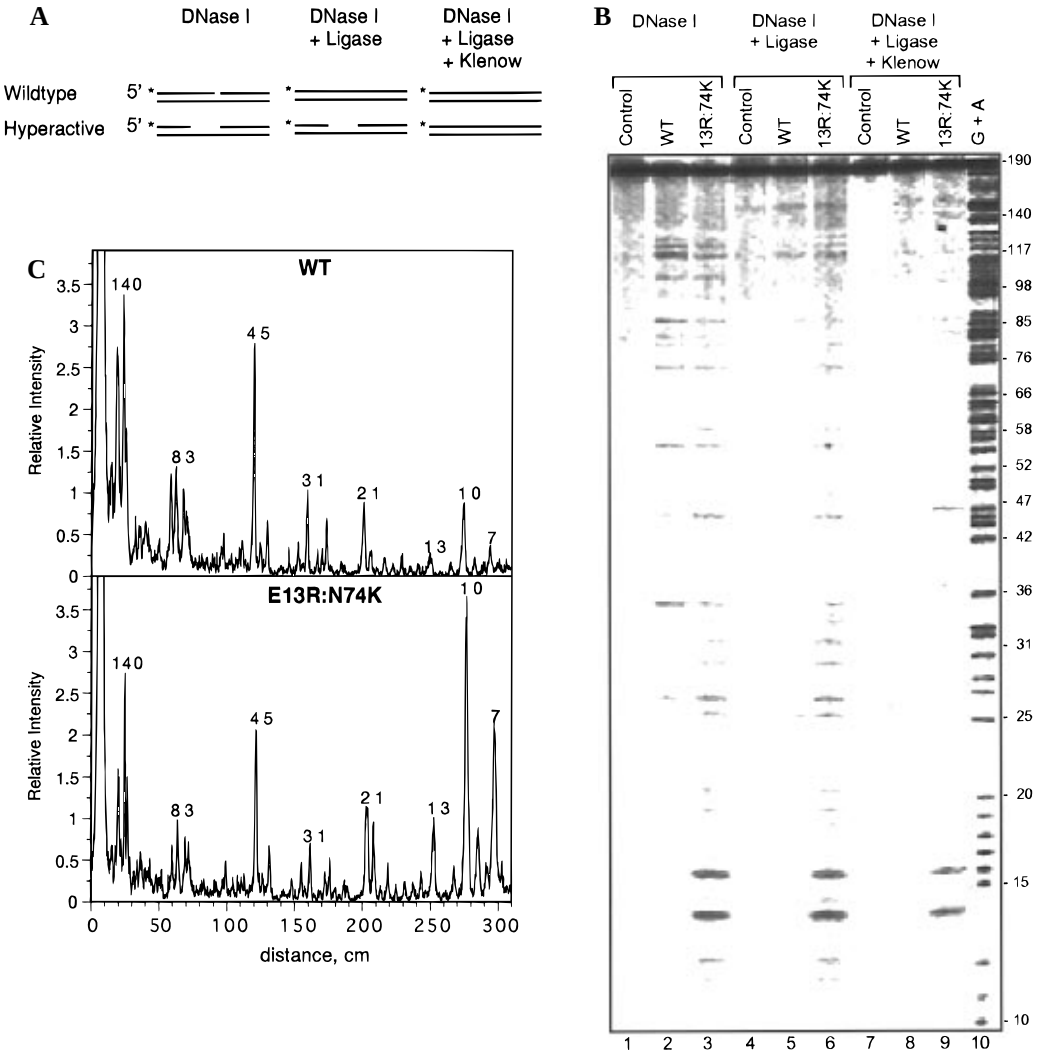

FIGURE 6: Digestion and repair of the end-radiolabeled 190mer *Eco*RI−*Ssp*I fragment. (A) Model of DNA digestion by wild-type and hyperactive DNase I and subsequent repair by ligase and the Klenow fragment of DNA polymerase I. (B) The 5′-end-labeled restriction fragment is treated with buffer control (lane 1, C), 2.5 ng/mL wild-type DNase I (lane 2, WT), or 0.1 ng/mL E13R:N74K mutant (lane 3, 13R:74K) for 5 min. The control and digested products are then repaired with T4 ligase in the absence (lanes 4−6) or presence (lanes 7−9) of the Klenow fragment of DNA polymerase I as described in Materials and Methods. All reactions were run on a 12% denaturing polyacrylamide gel followed by phosphoimager scanning to monitor the degradation pattern on the upper strand. The G + A marker is displayed on lane 10 with the size of DNA in nucleotides depicted on the right. (C) The 3′-end-labeled restriction fragment is treated with 1.5 ng/mL wild-type DNase I or 0.1 ng/mL E13R:N74K mutant as described in Materials and Methods. The relative intensity of each band is then plotted along the length of the gel, with some of the major peaks labeled according to their nucleotide size. Degradation by the wild-type and mutant enzyme resulted in 24.0% and 24.4% loss of the 190mer substrate, respectively. The intensity of the parent 190mer band is out of the range of this plot. Note that digestion with the hyperactive DNase I yields a greater proportion of lower molecular weight products than that with the wild type when both enzymes are used at identical overall nicking activity.

DISCUSSION

We have rationally designed hyperactive variants of human DNase I by replacing residues proximal to the DNA phosphate backbone with positively charged amino acids. The introduction of positively charged residues at sites distal from the DNA interface does not result in hyperactive variants (Ulmer et al., 1996), indicating that the engineered electrostatic interactions are specific and not global (Honig & Nicholls, 1995; Zhang et al., 1996). An increase in substrate affinity often does not lead to a more active enzyme. However, we have demonstrated the feasibility of this approach by taking advantage of the extremely weak substrate affinity of DNase I. Native human DNase I displays poor affinity to DNA. Surface plasmon resonance and gel-retardation studies showed no detectable DNA binding at up to 10 μM protein concentration (data not shown). The inability of this nuclease to tightly bind DNA may explain its single-stranded nicking mechanism. Arming it with additional basic residues allows it to remain on its substrate long enough to yield processive nicking of the same strand or nicking on the opposite strand at the same position, either of which functionally results in increased double-stranded DNA cleavage. Therefore, we have altered the functional or macroscopic mechanism of DNA degradation without inherently changing the catalytic machinery or microscopic mechanism at the active site.

Although the precise pathway of double-stranded DNA scission observed for the hyperactive variants is unclear, our data from the ligase and polymerase experiments (Figure 6A,B) support a processive nicking mechanism that results in the formation of DNA gaps (Figure 7). After initial single-stranded nicking, double-stranded DNA with its inherent low affinity for wild-type DNase I is likely released before any further degradation. However, the hyperactive variants with

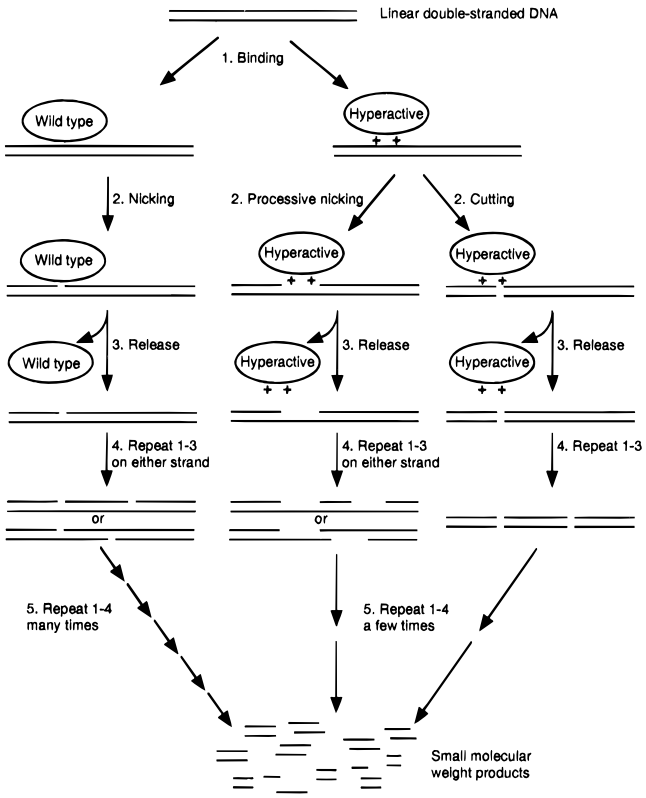

FIGURE 7: Proposed mechanisms of DNA digestion by wild-type and hyperactive DNase I. The + symbols represent the additional positive charges engineered into the hyperactive variants.

their additional positive charges may release the nicked DNA more slowly, allowing time for sliding along the minor groove of DNA and subsequent hydrolysis of adjacent phosphodiester bonds. Evidence for DNA sliding as a mechanism of specific recognition by DNA binding proteins has been established (Coleman & Pugh, 1995; Roberts & Halford, 1993; Ruusala & Crothers, 1992).

One model that is consistent with processive nicking by the hyperactive DNase I variants such as E13R:N74K involves an "inch-worming" mechanism. In the crystal structure of DNA−DNase I complex (Weston et al., 1992), the conformation of the DNA double helix is significantly strained by bending away from DNase I (Figure 1A). After nicking one strand, the wild type releases the nicked DNA completely; however, the hyperactive variant only partially releases the right half of the DNA binding site, holding onto the left half with the two additional positive charges at positions 13 and 74 (Figure 1A). The partial release may allow the nicked DNA to return to its native extended conformation, thus placing the next phosphodiester bond close to the active site. After reassociation by the right half and subsequent DNA bending to form the active enzyme−substrate complex, catalysis may again proceed. In this manner the stored energy created by DNA bending may help propel the hyperactive DNase I variant along the minor groove of DNA. The frequency at which the enzyme is completely released from the DNA at each nucleotide would govern the average size of the resulting single-stranded gaps, although nicking may not occur at every nucleotide. Additional experiments are needed to determine the gap size generated by the hyperactive DNase I and as well as to substantiate this model.

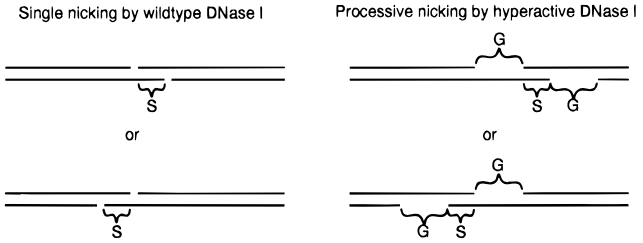

FIGURE 8: Model for the probability of observing a double-stranded DNA break. Let P_{nick} and P_{gap} be the probability of observing a double-stranded break from a given single hit on each strand for a nicking or gapping mechanism, respectively. Let L be the length of DNA, S be the separation between single-stranded breaks that results in a double-stranded break, and G be the gap size. Then, for $L \gg S$, $P_{nick} = (1/L)(2S/L)$ and $P_{gap} = (G/L)[(2S + G)/L]$, with $P_{gap}/P_{nick} = G[1 + G/(2S)]$. The $2S$ term is used because the second hit can be within a distance S in either direction of the first hit whereas only the G term is used because the gap produced can only go in one direction once the processive degradation starts. We also assumed that no digestion occurs directly opposite the first gap since DNase I highly prefers double-stranded DNA.

The probability of having double-stranded breaks is greater for DNA fragments containing single-stranded gaps than those with single-stranded nicks, especially when the gap size is large (Figure 8). This could explain the higher linear to relaxed product ratios generated by the hyperactive variants such as E13R, N74K, or E13R:N74K when compared to wild type (Figure 2A and Table 1). Alternatively, the hyperactive variants may utilize a mechanism involving individual nicks that are introduced in close proximity on both strands. After the initial nicking on the first strand, the variants, with their enhanced electrostatic interactions with DNA, would need to stay on the DNA long enough to rotate in a loose complex and subsequently nick the second strand (Figure 7). This mechanism is consistent with the fact that a few of the DNA fragments generated by digestion with the E13R:N74K hyperactive variant cannot be converted back to the initial substrate after treatment with Klenow and ligase (Figure 6B, lane 9); however, these fragments may also arise from overdigestion of the DNA. Finally, the positively charged residues may interact with the DNA in a fashion similar to that of divalent transition metal ions such as Mn^{2+} or Co^{2+}, which also enhance the double-stranded cutting pathway (Campbell & Jackson, 1980; Melgar & Goldthwait, 1968a,b). A model has been proposed suggesting that these transition metal ions promote double-stranded DNA cutting by altering the local conformation of the DNA and destabilizing the double helix (Campbell & Jackson, 1980). The three proposed mechanisms are not mutually exclusive, and it is possible the hyperactive variants may use all three.

The nicking activity of the E13R:N74K mutant is ~20 times higher than that of wild type when ~0.5 μg/mL radiolabeled 190mer restriction fragment was used as the substrate (Figure 6) but was ~2 fold lower than that of wild type when 30 μg/mL unlabeled linear pBR322 plasmid was used as the substrate (Figure 4). A possible explanation for these results involves a change in the rate-limiting step from association to dissociation as a function of increasing DNA concentration. The doubly positively charged mutant should have a faster association rate but a slower dissociation rate than the wild type. Another explanation could be that, in the absence of salt, both the K_m and the V_{max} for the nicking

activity of the mutant are lower than that of wild-type DNase I. Finally, as the mutant DNase I processively degrades DNA, it can slide off the ends of a shorter DNA fragment more quickly than a longer one, thus reducing its turnover time and yielding higher nicking activity, at least as measured by disappearance of the substrate.

Genetic selection for super repressor mutants has demonstrated that the introduction of positively charged amino acid side chains in the protein−DNA interface can increase the half-life of the protein−DNA complex (Hurlburt & Yanofsky, 1990; Nelson & Sauer, 1985; Tian & Maas, 1994). Our results show that this strategy can be applied toward an enzyme utilizing DNA as a substrate such that substantially altered functionality is imparted. This is probably a general phenomenon that could be applied to other nucleases as well. It is noteworthy that such a drastic change in functional activity can be accomplished by relatively few changes on the surface of this enzyme. The presence of DNase I in exocrine pancreatic secretions suggests a role as a digestive enzyme; however, its true physiological function remains unknown (Laskowski, 1971). As to why nature chose DNase I to degrade DNA by introducing nicks rather than gaps, we speculate that this may be a safeguard since DNA repair mechanisms could function better with nicked DNA.

We have coupled the K_m and V_{max} effects to generate a hyperactive DNase I variant that is ~35-fold more active than wild type. The addition of more positive charges could have a negative effect on activity under physiological saline concentrations *in vitro* since Q9R:E13R:N74K activity is optimal at 150 mM NaCl. However, *in vivo*, additional positive charges could facilitate the ability of DNase I to compete for DNA binding with histones and other DNA binding proteins.

The mutations described herein that create hyperactive variants are distinct from those that result in actin-resistant variants, which are 10−50 times more effective than wild type in degrading DNA in CF sputum (Ulmer et al., 1996). The enhanced activity predicted from the combination of hyperactivity with actin resistance in a single DNase I variant has great potential for CF therapy. In addition, Macanovic et al. (1996) have recently demonstrated that treatment in a murine model of systemic lupus erythematosus (SLE) with wild-type murine DNase I at the relatively high dose of 7.5 mg kg^{-1} day^{-1} prolonged murine survival by 30% as well as had beneficial effects on markers of renal function. Therefore, more potent versions of DNase I may prove valuable for the treatment of SLE as well.

ACKNOWLEDGMENT

We acknowledge C. Eigenbrot for molecular modeling, J. Ulmer, A. Herzka, D. Sinicropi, G. Lee, T. Dodge, R. Erickson, L. O'Connell, and H. Lowman for technical expertise and helpful discussions, Genentech's Assay Services Group for technical assistance, M. Vasser, P. Jhurani, and P. Ng for oligonucleotide synthesis, and D. Wood and L. Tamayo for graphics.

REFERENCES

Boat, T. F., Welsh, M. J., & Beaudet, A. L. (1989) in *The Metabolic Basis of Inherited Disease* (Scriver, C. L., Beaudet, A. L., Sly, W. S., & Valle, D., Eds.) pp 2649−2680, McGraw-Hill, New York.

Campbell, V. W., & Jackson, D. A. (1980) *J. Biol. Chem. 255*, 3726−3735.

Coleman, R. A., & Pugh, B. F. (1995) *J. Biol. Chem. 270*, 13850−13859.

Collins, F. S. (1992) *Science 256*, 774−779.

Cowan, R., Collis, C. M., & Grigg, G. W. (1987) *J. Theor. Biol. 127*, 229−245.

Doherty, A. J., Worrall, A. F., & Connolly, B. A. (1995) *J. Mol. Biol. 251*, 366−377.

Ferrin, T. E., Huang, C. L., Jarvis, L. E., & Langridge, R. (1988) *J. Mol. Graphics 6*, 13−27.

Fuchs, H. J., Borowitz, D. S., Christiansen, D. H., Morris, E. M., Nash, M. L., Ramsey, B. W., Rosenstein, B. J., Smith, A. L., & Wohl, M. E. (1994) *N. Engl. J. Med. 331*, 637−642.

Honig, B., & Nicholls, A. (1995) *Science 268*, 1144−1149.

Hurlburt, B. K., & Yanofsky, C. (1990) *J. Biol. Chem. 265*, 7853−7858.

Kotzin, B. L., & O'Dell, J. R. (1995) in *Samter's Immunologic Diseases* (Frank, M. M., Austen, K. F., Claman, H. N., & Unanue, E. R., Eds.) pp 667−697, Little, Brown and Co., Boston, MA.

Kunitz, M. (1950) *J. Gen. Physiol. 33*, 349−362.

Lachmann, P. J. (1996) *Clin. Exp. Immunol. 106*, 187−189.

Laskowski, M., Sr., (1971) in *The Enzymes* (Boyer, P. D., Ed.) pp 289−311, Academic Press, New York.

Liao, T. H., & Hsieh, J. C. (1988) *Biochem. J. 255*, 781−787.

Macanovic, M., Sinicropi, D., Shak, S., Baughman, S., Thiru, S., & Lachmann, P. J. (1996) *Clin. Exp. Immunol. 106*, 243−252.

Melgar, E., & Goldthwait, D. A. (1968a) *J. Biol. Chem. 243*, 4401−4408.

Melgar, E., & Goldthwait, D. A. (1968b) *J. Biol. Chem. 243*, 4409−4416.

Misra, V. K., Hecht, J. L., Sharp, K. A., Friedman, R. A., & Honig, B. (1994) *J. Mol. Biol. 238*, 264−280.

Nelson, H. C. M., & Sauer, R. T. (1985) *Cell 42*, 549−558.

Quinton, P. M. (1990) *FASEB J. 4*, 2709−2717.

Ramsey, B. W., Astley, S. J., Aitken, M. L., Burke, W., Colin, A. A., Dorkin, H. L., Eisenberg, J. D., Gibson, R. L., Harwood, I. R., Schidlow, D. V., Wilmott, R. W., Wohl, M. E., Meyerson, L. J., Shak, S., Fuchs, H., & Smith, A. L. (1993) *Am. Rev. Respir. Dis. 148*, 145−151.

Record, M. T., Jr., Anderson, C. F., & Lohman, T. M. (1978) *Q. Rev. Biophys. 11*, 103−178.

Roberts, R. J., & Halford, S. E. (1993) in *Nucleases* (Lin, S. M., Lloyd, R. S., & Roberts, R. J., Eds.) pp 52−53, Cold Spring Harbor Laboratory Press, New York.

Ruusala, T., & Crothers, D. M. (1992) *Proc. Natl. Acad. Sci. U.S.A. 89*, 4903−4907.

Sambrook, J., Fritsch, E. F., & Maniatis, T. (1989) *Molecular Cloning: A Laboratory Manual*, 2nd ed., Cold Spring Harbor Laboratory Press, New York.

Shak, S., Capon, D. J., Hellmiss, R., Marsters, S. A., & Baker, C. L. (1990) *Proc. Natl. Acad. Sci. U.S.A. 87*, 9188−9192.

Tian, G., & Maas, W. K. (1994) *Mol. Microbiol. 13*, 599−608.

Ulmer, J. S., Herzka, A., Toy, K. J., Baker, D. L., Dodge, A. H., Sinicropi, D., Shak, S., & Lazarus, R. A. (1996) *Proc. Natl. Acad. Sci. U.S.A. 93*, 8225−8229.

Weston, S. A., Lahm, A., & Suck, D. (1992) *J. Mol. Biol. 226*, 1237−1256.

Wolf, E., Frenz, J., & Suck, D. (1995) *Protein Eng. 8* (Suppl.), 79.

Zhang, W., Bond, J. P., Anderson, C. F., Lohman, T. M., & Record, M. T., Jr. (1996) *Proc. Natl. Acad. Sci. U.S.A. 93*, 2511−2516.

BI962960X